

Original Research

Experimental Study on Nonlinear Fluid Flow Characteristics of Fractured Granite Rocks Treated by Chemical Corrosion Under Confining Pressure Conditions

Richeng Liu¹, Zihan Li², Xuntu Yin¹, Xiaolin Wang^{1*}¹ China University of Mining and Technology, Xuzhou 221116, China² Shandong Experimental High School, Jinan 250109, China*Received: 1 December 2023**Accepted: 14 May 2024*

Abstract

This study aims to investigate the nonlinear fluid flow characteristics of fractured granites treated by chemical corrosion under confining pressure conditions. The granite samples with pre-existing fractures underwent chemical corrosion treatment with a $pH = 1\sim 12$ and corrosion durations of $t = 5\sim 100$ days. The nonlinear fluid flow tests were conducted under confining pressures $\sigma = 0.5\sim 20$ MPa. The results revealed that the pressure difference ($-\Delta P$) between the inlet and outlet increased with the increment of flow rate, while it decreased with increased σ . When $pH = 1$, $-\Delta P$ for the samples with $t = 100$ days of corrosion was 25% higher than that treatment with $t = 5$ days. When $pH = 3$ or 7 , $-\Delta P$ for the samples with $t = 100$ days was approximately twice that of the samples with $t = 5$ days. When $pH = 12$, $-\Delta P$ for the samples with $t = 100$ days was the same as that after treated with $t = 5$ days. The critical hydraulic gradient (J_c) that quantifies the onset of nonlinear fluid flow remained relatively constant when $pH = 7$, but it exhibited significant fluctuations when $pH = 1, 3$, or 12 . The permeability (K) decreased with increasing σ , and t had the most pronounced impact in neutral conditions. Predictive equations for J_c and K following chemical corrosion treatment were proposed and compared to experimental data, demonstrating a good fit between the two sets and verifying their validity. This study can provide criteria for quantifying fluid flow states and can accurately estimate the hydraulic properties of rock masses treated after chemical corrosion.

Keywords: Nonlinear fluid flow characteristics, chemical corrosion, water-rock interaction, permeability, hydraulic gradient

Introduction

The fluid flow characteristics of fractured rock masses under multi-field coupling conditions are of great importance

for underground engineering [1–3]. The groundwater seriously affects the mechanical behavior of surrounding rocks and the stability of underground engineering [4–7]. Under the influence of solute and mineral composition, groundwater is often acidic or alkaline to varying degrees, which produces long-term chemical corrosion on fractured rock masses [8, 9].

*e-mail: wangxiaolin@cumt.edu.cn

Chemical corrosion will reduce rock strength due to the change in the skeleton properties of rock particles and the increase in pores. Li et al. [10] conducted direct shear tests of granite samples under dry, wet, and saturated conditions. The deterioration of rocks under saturated conditions was the most obvious. Kessler et al. [11] conducted 116 uniaxial compression tests of granites and found that the uniaxial compressive strength of waterlogged specimens decreased by 12% compared with that of dry specimens. Luo et al. [12] used a soil acid solution to analyze the mechanical and hydraulic properties of granite samples with prefabricated fractures under chemical corrosion conditions. The results show that in order to improve the hydraulic properties of the samples, appropriate chemical reagent types, reaction times, and reagent doses should be used. Xu et al. [13] simulated the change in fluid flow characteristics of granites under chemical corrosion using TOUGHREACT software. The results show that the higher the pH value of the chemical solution, the higher the porosity and the larger the permeability of granite fractures. Farquharson et al. [14] conducted fluid flow tests on granite samples containing fracture networks and found that acid stimulation with different concentrations of hydrochloric acid can effectively improve the porosity and permeability of fractured rock masses. Feng et al. [15] carried out corrosion treatment experiments on granite with different chemical solutions. The results showed that the connection between mineral particles was disturbed under the action of chemical solution corrosion, which significantly reduced the strength of rocks by causing damage to rock structures.

There are also extensive studies on the impact of chemical corrosion duration on the mechanical properties of fractured rock masses [16, 17]. Shang et al. [18] soaked granite samples with prefabricated fractures in an acid solution for 150 days, and the results showed that, compared with dry samples, the strength of fractured granite samples after soaking for 150 days was decreased by 12.1%. Sheng et al. [19] conducted a shear test on the limestone samples after drying and water soaking for 120 hours. The study showed that the roughness of the internal fracture surface of the samples after 120 hours of water soaking increased, and the peak shear strength increased by 8.83% on average, while the residual shear strength did not change much. Huang et al. [20] considered the chemical corrosion of surrounding rocks in tunnels, such as granite, sandstone, and marble, in an acidic Na_2SO_4 solution for 7 days. They found that acid corrosion made the rock surface broken, and the surface roughness increased significantly. Meng et al. [21] carried out fluid flow tests of fractured rock masses under different confining pressures. They found that with the increase in confining pressure, the permeability of rock samples decreased and the nonlinear flow coefficient increased. Fu et al. [22] studied the influences of confining pressure and fracture roughness on fluid flow characteristics. They found that with the gradual increase in confining pressure, the permeability appeared in two stages with rapid and slow reductions, respectively. When the confining pressure was greater than 50 kPa, this trend gradually disappeared. In

the process of underground engineering construction, fractured rock masses are often subjected to the actions of confining pressure and chemical corrosion. Thus, water-rock interaction, chemical corrosion, and confining pressure have complicated effects on fluid flow through rock masses.

The above research mainly focuses on the impact of chemical corrosion on the physical and mechanical properties of rocks. A few studies have focused on the influence of chemical corrosion on the hydraulic properties of single fractures. However, the hydraulic properties of fracture networks within granites treated after chemical corrosion through experiments have not been investigated, if any. Besides, the nonlinear fluid flow characteristics of fracture networks within granites treated after chemical corrosion were also not taken into account. Thus, the critical hydraulic gradient that quantifies the onset of nonlinear flow cannot be determined, and the permeability of fractured rock masses with high hydraulic pressure cannot be accurately estimated.

The objective of this study is to investigate the effects of water-rock interaction, chemical corrosion, and confining pressure on the nonlinear flow characteristics of fluids through fractured rock masses treated after chemical corrosion. First, a total of 8 standard samples of granite containing prefabricated fractures are immersed in chemical solutions with pH values of 1, 3, 7, and 12, for soaking times t of 5 days and 100 days, respectively. Then, fluid flow tests were carried out on the chemically etched specimens, and the confining pressure σ was set to 0.5 MPa, 3 MPa, 5 MPa, 10 MPa, and 20 MPa, respectively. Next, the relationships between the volume flow rate Q and the pressure difference $-\Delta P$ between the inlet and outlet are obtained. The influences of pH value, t , and σ on the nonlinear fluid flow characteristics of fractured rock mass are analyzed. Finally, the critical hydraulic gradient and permeability prediction equations are proposed, which can provide criteria for quantifying the fluid flow states and can accurately estimate the hydraulic properties of rock masses treated after chemical corrosion.

Material and Methods

The study was designed in four steps. First, the granite samples were prepared and saw-cut to form connected fracture networks. Then, these samples were treated in solutions with different pH values, which can change the mechanical and hydraulic properties of the samples. Next, nonlinear fluid flow tests were carried out on the chemically treated samples. Finally, the governing equations of fluid flow were introduced to analyze the nonlinear fluid flow behaviors. The study was carried out through experiments and theoretical analysis. The data were analyzed after obtaining the relationships between volumetric flow rate and hydraulic pressure on samples treated after chemical corrosion under different confining pressures. The nonlinear factors in Forchheimer's law are analyzed, and the critical hydraulic gradient that quantifies the onset of nonlinear fluid flow is calculated. The predictive

equations of critical hydraulic gradient and permeability are proposed, which have great scientific contributions to understanding the hydraulic properties of fractured rock masses treated after chemical corrosion.

Specimen Preparation

A total of 8 cylindrical granite samples with a height of 100 mm and a diameter of 50 mm were used, and the main mineral compositions were 49% plagioclase, 42% quartz, and 6% mica. The granite samples used are bulk purchased rock samples with uniform mineral composition, and the influence of rock inhomogeneity is very small, so a parallel test is not needed. Based on the complexity of the geometric features of natural joints, we use a rock engraving machine to conduct a unified precast fracture treatment on all standard granite samples

to obtain the same fracture network geometry. The aperture of each fracture is 4 mm, thus forming a granite fractured rock mass with connected fluid flow channels as shown in Fig. 1 (a). The internal fracture network is shown in Fig. 1 (b). The geometric characteristics of fracture networks for all samples are completely consistent.

Chemical Corrosion Treatment

The granite samples with prefabricated fractures were divided into 4 groups and placed into 4 containers of distilled water. The 12 mol/L concentrated hydrochloric acid was slowly added to the first set of distilled water, and a *pH* test pen was used to measure the *pH* value. The chemical solution was controlled with a *pH* = 1, in which the chemical solution fully covered the sample. The above procedure for the second set of distilled water was repeated by controlling

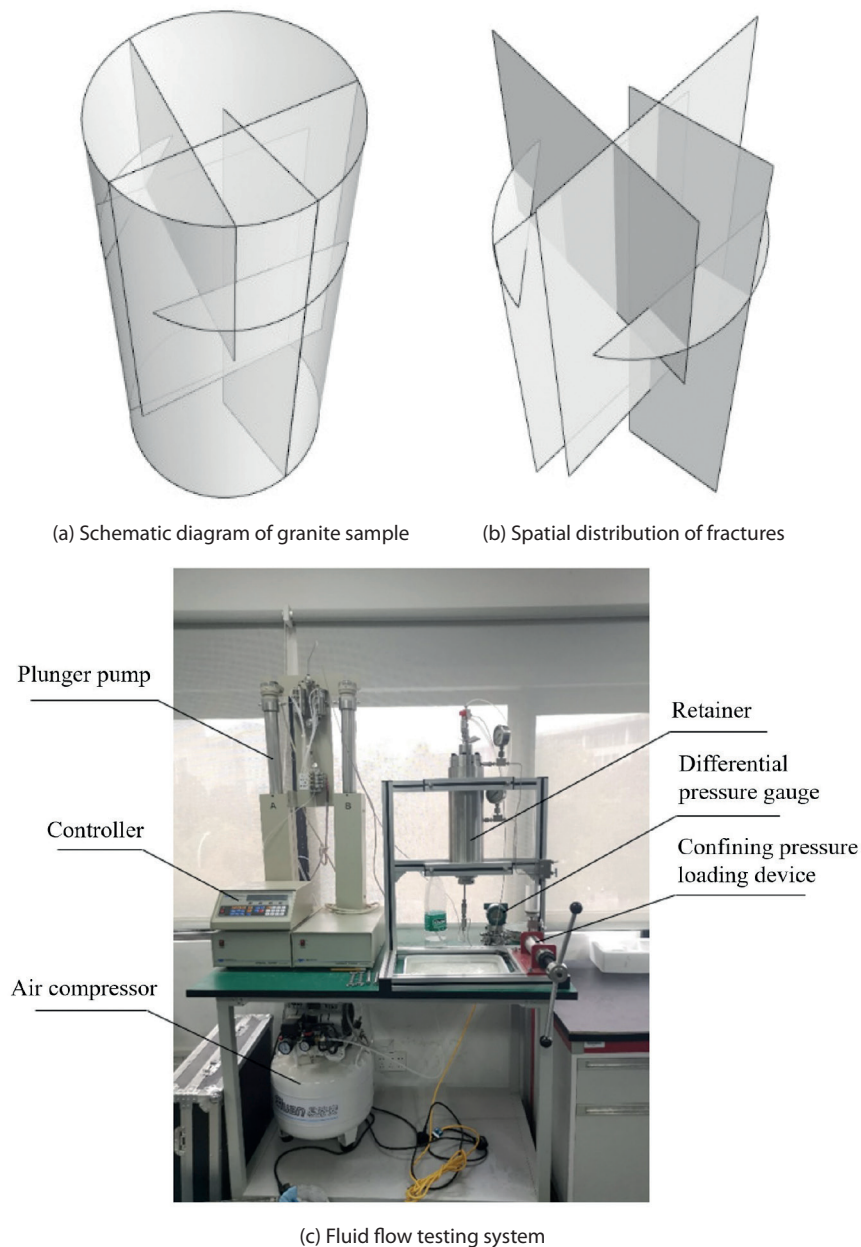


Fig. 1. Schematic view of granite samples containing connected fractures, and fluid flow testing system

the chemical solution with a $pH = 3$. The third group of distilled water remained the same with a $pH = 7$, while serving as the reference group. Solid NaOH was added to the fourth set of distilled water solutions and stirred until $pH = 12$. Concentrated hydrochloric acid or solid NaOH is added daily to the corresponding chemical solution throughout the immersion test to maintain a constant pH . Chemical corrosion tests are carried out in a fume hood at room temperature to minimize the influence of temperature on the interaction between the solution and the sample. After soaking for 5 days, one sample was removed from each group of containers for fluid flow tests, and the remaining samples were soaked in a chemical solution for 100 days before being taken out for the other fluid flow tests.

Fluid Flow Tests

The high-precision pulse-free long-time penetration test system was adopted for the tests, as shown in Fig. 1(c). The experimental system mainly includes a water inlet device, a sample holding device, a constant speed, and constant pressure pump pressure device, and a data acquisition and processing system in which the fluid flow pump can be used with the computer to set remote parameters, save data, and perform other operations. The fluid flow testing system mainly has two working modes: constant pressure mode and constant flow rate mode. The measurement accuracy of hydraulic pressure difference is 0.001 kPa, and the accuracy of flow rates is 0.01 ml/min. During the test, the sample is placed in the pressure chamber, which can apply different axial pressures and confining pressures. The maximum confining pressure and axial pressure are both 60 MPa.

Before the fluid flow test, the sample is first saturated with water to ensure that water can fill and flow through the sample quickly. At the beginning of the test, the air pump valve of the air compressor should be opened. Then, the fluid flow pump was opened. The sample was placed in the pressure chamber, and the screw cap at the water inlet was tightened. Next, the fluid flow pump and the pressure chamber were connected, and the axial pressure of approximately 1 MPa was applied to the sample before applying the confining pressure. When the confining pressure is applied to a predetermined value, the confining pressure valve is closed so that the sample is tested under constant confining pressure conditions. Finally, the inlet volume flow rate is set through the operation panel. After the inlet pressure is stable, the data is read and saved, and then the confining pressure valve with a new value is opened again. Fluid flow tests with confining pressures of 0.5 MPa, 3 MPa, 5 MPa, 10 MPa, and 20 MPa are carried out, respectively. In each case, Q ranges from $3.33 \times 10^{-7} \text{ m}^3/\text{s}$ to $1.83 \times 10^{-6} \text{ m}^3/\text{s}$. Detailed parameters and results are listed in Table 1. All the fluid flow tests were carried out at room temperature at about 20°C . Newtonian incompressible fluid with density ρ of 1000 kg/m^3 and a dynamic viscosity coefficient μ of $1.003 \times 10^{-3} \text{ Pa}\cdot\text{s}$ was used in the test. A low Q is set, and the test data is recorded after the pressure difference $-\Delta P$ is stabilized.

The relationship between Q and hydraulic gradient J is obtained through calculation, and subsequent parameters such as linear and nonlinear coefficients in Forchheimer's law are calculated. The influences of pH , t , and σ on the fluid flow characteristics of rock fractures were analyzed.

Governing Equations

As a viscous incompressible Newtonian fluid, the flow of water in rough fractures can be expressed by the Navier-Stokes (N-S) equation [23]:

$$\rho [\partial \mathbf{u} / \partial t + (\mathbf{u} \cdot \nabla) \mathbf{u}] = -\nabla \mathbf{P} + \nabla \cdot \mathbf{T} + \rho \mathbf{f} \quad (1)$$

where \mathbf{u} is the flow velocity tensor, ρ is the fluid density, \mathbf{P} is the hydraulic pressure tensor, \mathbf{T} is the stress tensor, t is the time, \mathbf{f} is the body force tensor, and ∇ is the Hamiltonian operator. The N-S equation is widely used, while the effects of fracture geometry and fluid inertia force change are taken into account. Eq. (1) is suitable for characterizing both linear and nonlinear flow behaviors in fluids. However, directly solving the N-S equation is a very time-consuming task and requires solving a set of differential equations. Therefore, a new equation to express the nonlinearity of fluid flow, namely the Forchheimer equation, was proposed, whose expression is written as follows [23]:

$$-\Delta P = aQ + bQ^2 \quad (2)$$

where a and b are the linear and nonlinear coefficients, and Q is the volume flow rate. aQ and bQ^2 represent the linear and nonlinear terms of fluid flow, respectively, which are related to the equivalent hydraulic aperture, roughness, and geometry of the fracture. When Q is small, the fluid is relatively stable, and the inertia force is much smaller than the viscous force. Q and $-\Delta P$ are linearly correlated and are in line with the Darcy linear flow, in which the nonlinear term bQ^2 can be ignored.

Permeability K is a coefficient used to characterize the fluid flow through rock fractures or fracture networks, as follows:

$$K = -\frac{\mu}{\nabla P} Q \quad (3)$$

Zeng et al. [24] defined a proportional coefficient E to characterize the flow state of fluid in fractured rock masses through a large number of laboratory tests and theoretical deduction, written as:

$$E = \frac{bQ^2}{aQ + bQ^2} \quad (4)$$

E is a dimensionless parameter in the range of 0 to 1. When studying the nonlinear fluid flow characteristics of fractured rock masses, Zimmerman et al. [25] adopted $E = 0.1$ as the critical value to quantify the onset of nonlinear fluid flow in fractured rock masses. When $E < 0.1$, $a/b < 0.9Q$, indicating that the ratio of the pressure gradient drop caused

Table 1. Experimental cases with different pH and different t, and associated results

NO.	pH	t (d)	σ (MPa)	a (Pa·s·m ⁻⁴)	b (Pa·s ² ·m ⁻⁷)	K (m ²)	J _c
1	1	5	0.5	2.65E+09	2.33E+15	1.92E-12	0.37
			3	5.06E+09	1.22E+15	1.01E-12	2.59
			5	5.10E+09	1.55E+15	9.99E-13	2.07
			10	7.01E+09	1.35E+15	7.27E-13	4.49
			20	7.21E+09	2.20E+15	7.07E-13	2.92
2	1	100	0.5	4.35E+09	1.42E+15	1.17E-12	1.65
			3	4.94E+09	1.72E+15	1.03E-12	1.75
			5	5.46E+09	1.77E+15	9.33E-13	2.08
			10	6.17E+09	2.36E+15	8.26E-13	1.99
			20	8.05E+09	3.28E+15	6.33E-13	2.44
3	3	5	0.5	4.46E+09	1.05E+15	1.14E-12	2.34
			3	4.97E+09	1.53E+15	1.03E-12	1.99
			5	5.11E+09	1.66E+15	9.97E-13	1.94
			10	5.72E+09	2.41E+15	8.91E-13	1.68
			20	5.35E+09	3.60E+15	9.52E-13	0.98
4	3	100	0.5	3.22E+09	4.21E+14	1.58E-12	3.04
			3	3.88E+09	5.23E+14	1.31E-12	3.55
			5	4.23E+09	3.72E+14	1.20E-12	5.94
			10	4.38E+09	5.35E+14	1.16E-12	4.43
			20	4.86E+09	6.20E+14	1.05E-12	4.70
5	7	5	0.5	1.70E+09	5.65E+14	3.00E-12	0.63
			3	1.83E+09	6.30E+14	2.78E-12	0.66
			5	1.91E+09	6.08E+14	2.67E-12	0.74
			10	1.95E+09	7.66E+14	2.61E-12	0.61
			20	2.33E+09	7.49E+14	2.19E-12	0.89
6	7	100	0.5	1.87E+09	7.95E+14	2.72E-12	0.54
			3	2.78E+09	1.38E+15	1.83E-12	0.69
			5	2.99E+09	1.41E+15	1.70E-12	0.78
			10	3.33E+09	1.43E+15	1.53E-12	0.96
			20	3.75E+09	1.69E+15	1.36E-12	1.03
7	12	5	0.5	2.05E+09	6.14E+14	2.49E-12	0.84
			3	2.28E+09	6.21E+14	2.23E-12	1.03
			5	2.36E+09	5.90E+14	2.16E-12	1.17
			10	2.36E+09	6.89E+14	2.16E-12	1.00
			20	2.70E+09	7.75E+14	1.89E-12	1.16
8	12	100	0.5	2.58E+09	2.51E+14	1.98E-12	3.27
			3	2.69E+09	2.25E+14	1.89E-12	3.97
			5	2.61E+09	3.73E+14	1.95E-12	2.25
			10	3.07E+09	2.72E+14	1.66E-12	4.28
			20	3.18E+09	5.28E+14	1.60E-12	2.36

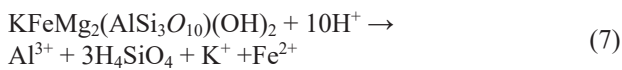
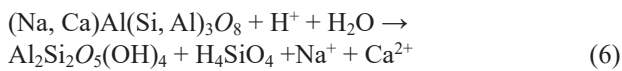
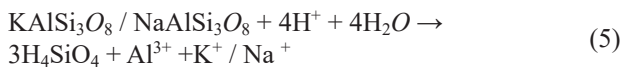
by the nonlinear term to the total pressure gradient drop is small (i.e., less than 10%), and the fluid is in the linear flow regime. When $E > 0.1$, $a/b > 0.9Q$, indicating that the ratio of the pressure gradient drop caused by the nonlinear term to the total pressure gradient drop is large (i.e., larger than 10%), and the fluid is in the nonlinear flow regime.

Results and Discussion

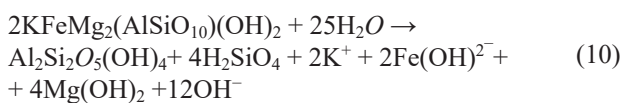
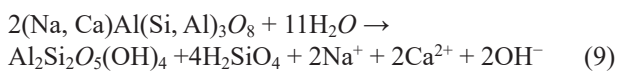
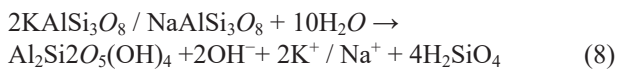
The pH values t and σ have significant influences on the surface morphology and fluid flow characteristics of fractured rock masses. The basic parameters for fluid flow tests and associated results are shown in Table 1.

Surface Morphology and Fragmentation of Rock Masses After Tests

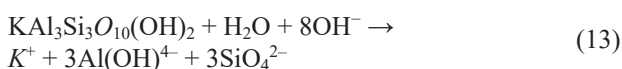
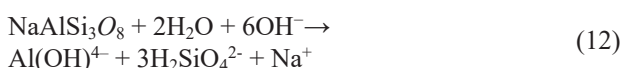
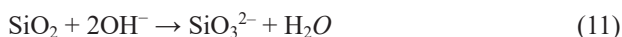
For rock samples in an acidic solution, the chemical reactions include feldspar dissolution and biotite dissolution [26]:



For rock samples in neutral solutions, the chemical reactions are feldspar dissolution and biotite dissolution:



For rock samples in alkaline solution, the chemical reactions are:



Due to water-rock interaction and chemical corrosion, the surface morphology of granite samples varies with different pH values and soaking times [27]. When pH is constant, the surface roughness of the sample with t

= 100 d increases significantly with respect to the sample with $t = 5$ d. This is because different minerals dissolve at different rates in chemical solutions, and the distribution of minerals on the granite surface is uneven. The surface minerals of the sample with $t = 100$ d react more fully with the chemical solution than those with $t = 5$ d. When t is constant, the surface roughness of the sample corroded by strong acid solution ($pH = 1$) and strong alkali solution ($pH = 12$) increases significantly, which indicates that the higher the concentration of the chemical solution, the more intense the reaction between the sample and chemical solution. Fig. 2(a)~(h) shows the failure of the sample after the fluid flow test. There is no significant difference in the degree of granite fragmentation with pH value, which is because the failure of fractured rock masses is mainly affected by their own structural characteristics [28]. When σ increases to 20 MPa, all the samples fracture at the intersection and end of the fracture due to the consistency of the preset fracture network. The characteristics, such as JRC, of the fractured rock samples produced are generally the same, so the influence of chemical corrosion cannot be directly observed from the broken phenomenon [29]. In Fig. 2(i)~(j), when t is constant, the granite surface color gradually turns from pure to yellow with the increment of acidity or alkalinity. When the pH value is constant, the larger the t , the more obvious the color of the sample surface and the corrosion effect. This indicates that the influences of the pH concentration of the chemical solution and the soaking time on granite cannot be ignored.

Nonlinear Fluid Flow Characteristics

Fig. 3 describes the relationships between $-\Delta P$ and Q , and zero-intercept regression fitting is obtained based on Eq. (4). The results show that the fluid flow test results under different σ agree with the Forchheimer theoretical equation, and the fitting coefficients R^2 are greater than 0.99. When pH , t , and Q are constant, $-\Delta P$ increases with the increase in σ . This is because the prefabricated fractures fail and are closed under the action of σ , and the internal fluid flow channels and hydraulic openness are reduced [30]. At the same time, the contact areas between the upper and lower surfaces of fractures are increased, and backflow and eddy currents are easily formed during the flow processes, resulting in energy losses [31].

When σ and Q are constant, the variations in $-\Delta P$ versus corrosion time are different in chemical solutions with different pH values. When the solution is neutral or weakly acidic ($pH = 3$ or 7), as shown in Fig. 3(c), (d), (e), and (f), the $-\Delta P$ at $t = 100$ d is twice the $-\Delta P$ at $t = 5$ d. This indicates that in the same external environment, the longer the corrosion time, the greater the pressure difference. In weakly acidic environments, chemical corrosion is dominated by water-rock interaction, and the granite softens and expands, compressing the original fracture channel and causing the pressure difference to increase [32]. When $t = 100$ d, long-term immersion results in a decrease in the compressive strength of rock masses, and the damage and deterioration to fractured rock masses are obvious.

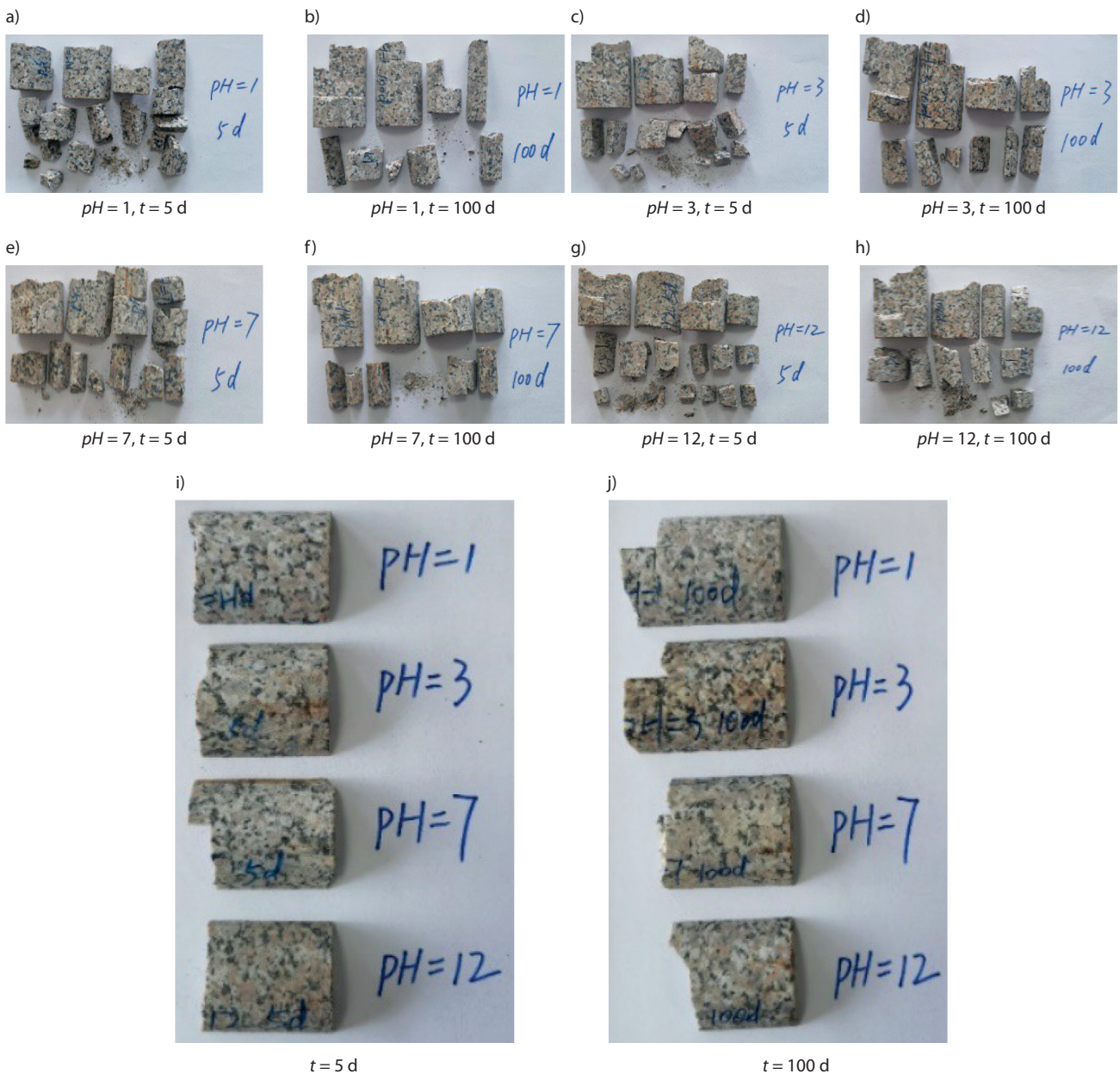


Fig. 2. Fragmentation distributions and the biggest block of granites after tests under solutions with different pH values and different soaking times.

Therefore, under the same pH , σ , and Q conditions, the greater t is, the more obvious $-\Delta P$ is increased.

When the solution is strongly acidic ($pH=1$), as shown in Fig. 3(a) and (b), $-\Delta P$ at $t=100$ d is 25% larger than $-\Delta P$ at $t=5$ d because H^+ in the chemical solution reacts with silicate minerals (such as feldspar and biotite) on the surface of the granite. Since the granite porosity is only about 0.2%, it is difficult for the chemical solution to enter the sample. Therefore, the soluble substance on the fracture surface will no longer react, which means that the degree of acid corrosion is not affected by time. Compared with neutral and weakly acidic solutions, $-\Delta P$ increases less with an increase in t . This is because when the strong acidic solution softens the rock sample

and improves the pressure difference, it will also provide a large amount of H^+ in the solution. The chemical reaction with the granite fracture surface makes the original fracture channel large. The numbers and lengths of fractures in the rock mass increase and the fluid flow channel increases due to the water-rock interaction [33], which improves the permeability of the fracture network to some extent so that the $-\Delta P$ increase in the strong acid solution is smaller than that of the weak acid solution.

When the solution is alkaline with a $pH=12$, the change in $-\Delta P$ after 100 days of corrosion is comparable to that after 5 days. This similarity arises from the stability of the reaction between the chemical solution at $pH=12$, and the granite minerals are attributed to the abundant presence of OH^- ions

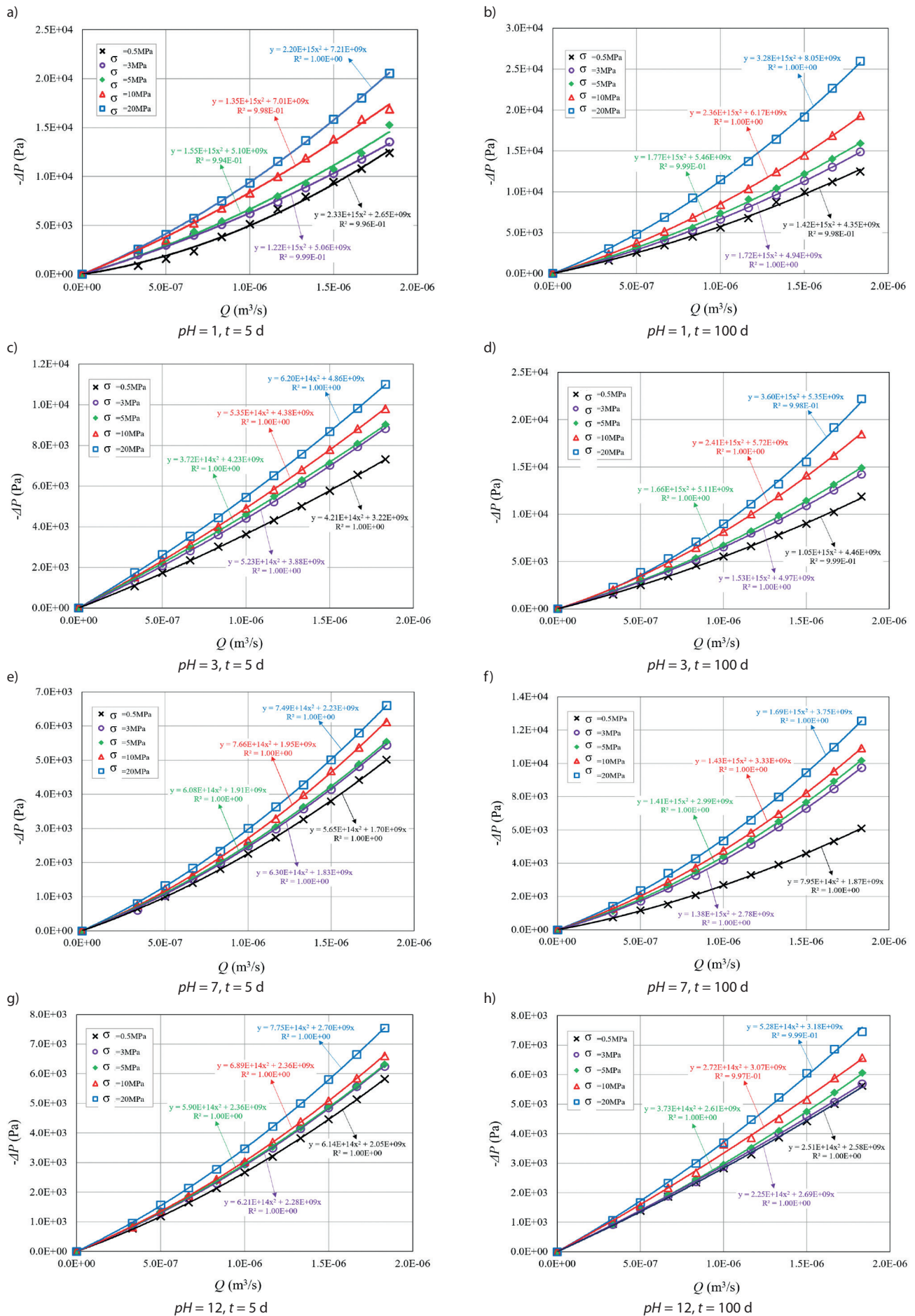


Fig. 3. Relationships between flow rate and pressure difference between inlet and outlet under different pH values and different soaking times.

in the solution. The NaOH solution interacts with silicate minerals like feldspar and mica, leading to the formation of a substantial amount of cementation material adhering to the fracture surface. This material effectively obstructs the fluid flow channels [34]. Consequently, the degree of fracture closure is nearly identical for both time intervals, $t = 5$ days and $t = 100$ days, resulting in roughly equivalent values for $-\Delta P$ in both instances.

The influence of σ on parameters a and b is depicted in Fig. 4. As σ increases from 0.5 MPa to 20 MPa, both a and b exhibit logarithmic growth. When σ surpasses 3 MPa, it becomes evident that b is six orders of magnitude larger than a . When we take Q as the maximum value, the assertion $> 0.9 Q$ holds true even when σ surpasses 3 MPa. Consequently, in scenarios where σ remains below 3 MPa, fluid flow predominantly adheres to a linear pattern. When σ exceeds 3 MPa, nonlinearity significantly impacts the fluid flow.

By substituting $E = 0.1$ into Eq. (6), the critical volume flow Q_c can be obtained. By substituting Q_c into Fig. 3, the corresponding critical inlet and outlet pressure differences can be obtained. Further calculation results of the critical hydraulic gradient J_c can be obtained as shown in Table 1 and the change in J_c with σ is shown in Fig. 5(a)~(d). When $pH = 1$, J_c of $t = 5$ d is greater than J_c of $t = 100$ d. When $pH = 3$, J_c of $t = 5$ d is smaller than J_c of $t = 100$ d. When $pH = 7$, J_c of $t = 5$ d is the same as J_c of $t = 100$ d. At $pH = 12$, the J_c of $t = 100$ d is three times the J_c of $t = 5$ d. It shows that in a neutral solution, J_c is not sensitive to t , and in acidic and alkaline solutions, J_c fluctuates up and down under the influences of t and σ . In an extremely acidic environment ($pH = 1$), the J_c at $t = 5$ days is larger than the J_c at $t = 100$ days. This suggests that under extreme acidity conditions, fluid flow behavior exhibits a pronounced sensitivity to time, with J_c decreasing over a long duration [35]. When the pH is moderately acidic ($pH = 3$), the J_c at $t = 5$ days is lower than the J_c at $t = 100$ days. This observation indicates that in a moderately acidic solution, the effect of t is reversed, with J_c increasing over an extended period. In a neutral solution ($pH = 7$), the J_c values at $t = 5$ days and $t = 100$ days are identical. This suggests that under neutral conditions, J_c remains relatively insensitive to the duration of exposure, implying stability over time. In a highly alkaline environment ($pH = 12$), the J_c at $t = 100$ days is three times greater than the J_c at $t = 5$ days. This demonstrates that in an alkaline solution condition, fluid flow behavior exhibits significant sensitivity to t , with J_c increasing substantially over a long period.

Evolution of Permeability

Figs. 5(e)~(h) show the influence of σ on permeability coefficient K under the action of different pH values and t . With the increase in σ , K gradually decreases, and the decline rate shows a trend of first fast and then slow. This is because the fracture network of prefabricated granite can produce large closures under small confining pressure. With the gradual increase in σ , the fracture closure degree gradually becomes stable [36].

Compared with $pH = 3$, when $pH = 7$, the K values of $t = 100$ d and $t = 5$ d show the most obvious difference, indicating that water-rock interaction is greatly affected by t and chemical corrosion is less affected by t . When σ and t are constant, the K after acid treatment is the smallest, and the K after neutral and alkaline solution treatments is the same. This is because during acid corrosion treatment, the soluble substance on the fracture surface reacts with H^+ in the chemical solution, resulting in the fracture surface becoming rougher. At the same time, the rock mass protruding from the rough surface softens and expands. Under the action of σ , the closure of fractures increases, resulting in a decrease in K . When the alkaline solution is treated, the strength of granites is reduced by water-rock interaction. Meanwhile, OH^- in a chemical solution reacts with silicate minerals on the surface of granites and produces cement precipitation, which plays a supporting and filling role when the fractures are closed.

Empirical Prediction Models of J_c and K

To quantitatively assess the effects of t , pH , and σ on both J_c and K , we employed databases containing values of t , pH , and σ to formulate four empirical equations based on deep learning techniques as follows:

When t is equal to 5 days, Eqs. (14) and (15) can be used to predict J_c and K :

$$J_c = 0.0304 \times (1.4948 + pH) \times e_1 \tag{14}$$

where:

$$e_1 = e^{(2.6787 \times \log(\frac{11.7605 + \sigma}{1.4948 + \sqrt{pH}}) - 1.5201)}$$

$$K = 5.1965 \times 10^{-8} \times (134.7121 + \sigma) \times e_2 \tag{15}$$

where:

$$e_2 = e^{(\frac{0.1109 \times (134.7121 + \sigma)}{-24.5972 + \log(pH)} + 0.0889 \times e^{pH} - 15.0553)}$$

When t is equal to 100 days, Eqs. (16) and (17) can be used to predict J_c and K :

$$J_c = 0.2917 \times (3.7617 + pH) \times e_3 \tag{16}$$

where:

$$e_3 = e^{(\frac{277.4366pH}{3.6717 \times (-62.8943 + \sigma)} + 0.2293)}$$

$$K = 6.0460 \times 10^{-7} \times (7.5027 + pH) \times e_4 \tag{17}$$

where:

$$e_4 = e^{(\frac{144.5664 \times (7.5027 + \sigma)}{20.2093 + pH} + 15.9665)}$$

These equations provide a robust framework for predicting J_c and K under various conditions of t , pH ,

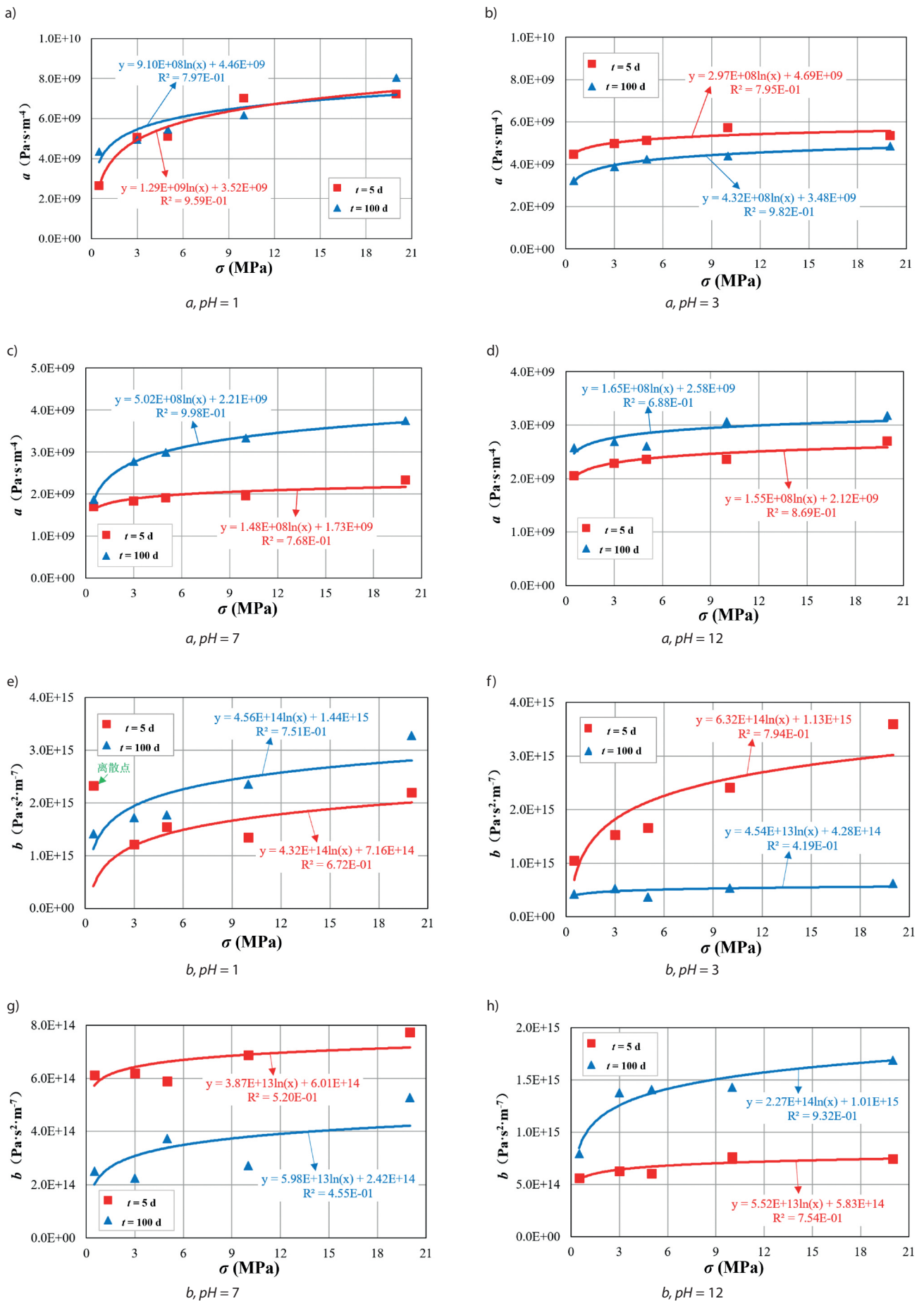


Fig. 4. Evolutions of linear coefficient a and nonlinear coefficient b versus confining pressure σ .

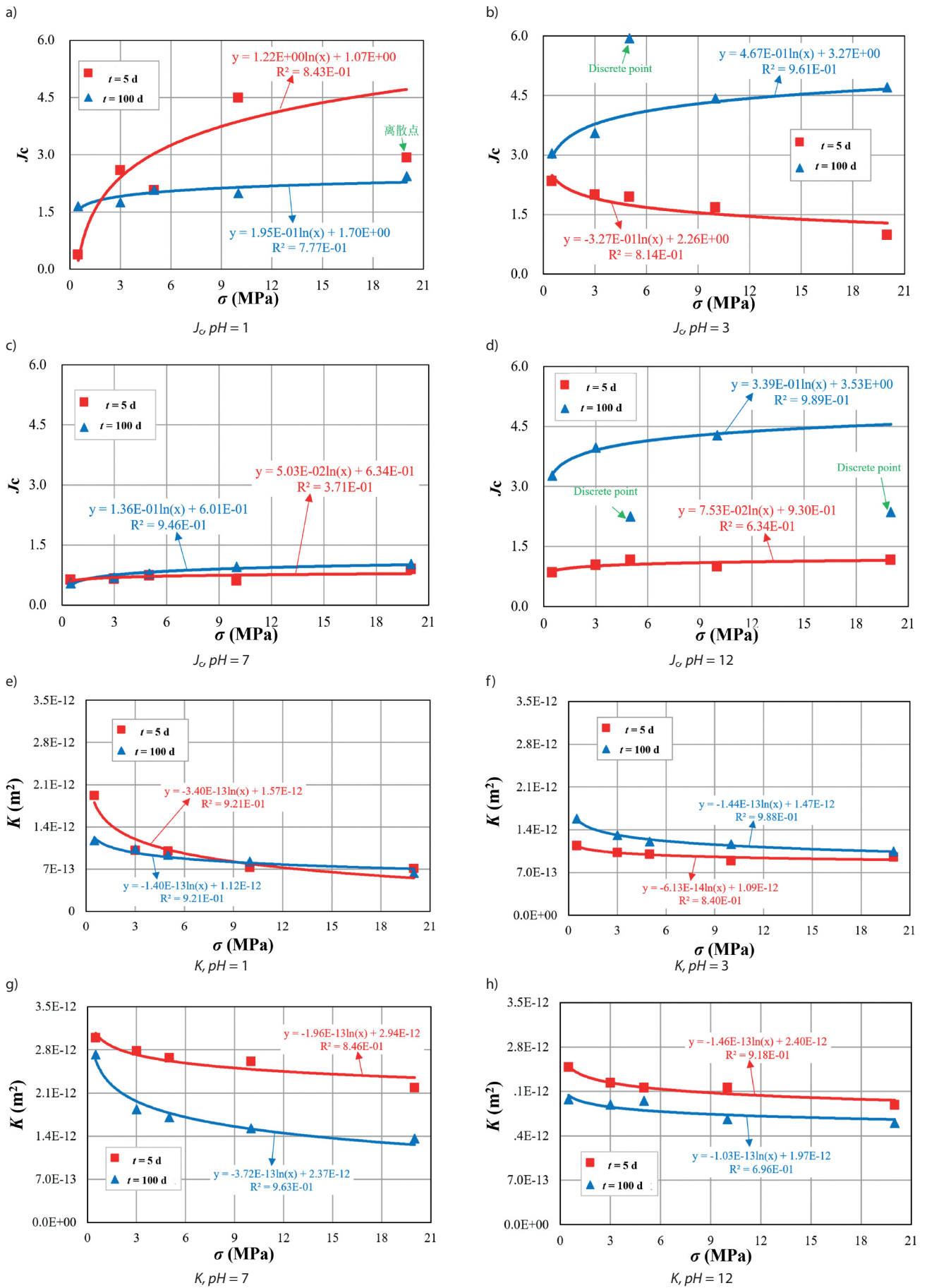


Fig. 5. Evolutions of critical hydraulic gradient J_c and permeability K versus confining pressure σ .

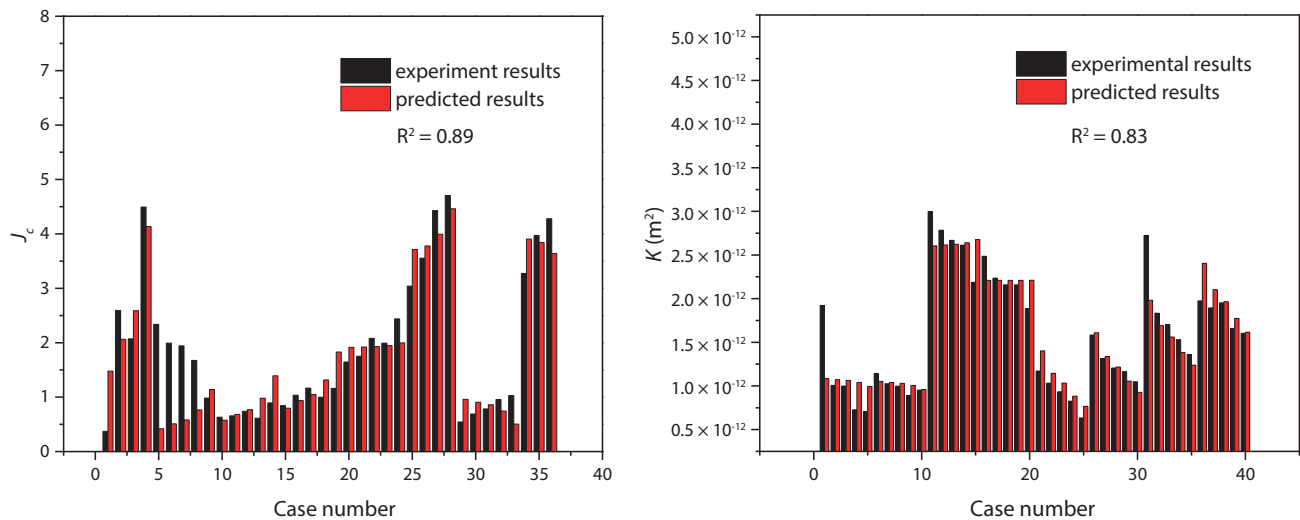


Fig. 6. Comparisons between experimental results and calculated results in the present study: (a) critical hydraulic gradient J_c , and (b) permeability K .

and σ , offering valuable insights into the relationships between these parameters and the fluid flow properties. As shown in Fig. 6, the experimental results are compared to the results obtained by calculating Eqs. (14)~(17). The experimental and calculated results are in good agreement, with $R^2 > 0.8$, demonstrating the accuracy and reliability of the equations that can be used to predict the hydraulic properties of fractured rock masses.

Conclusions

In this study, the nonlinear fluid flow characteristics of fractured rock masses under different confining pressures (0.5, 3, 5, 10, 20 MPa) and different chemical environments were investigated. Fluid flow experiments of granite samples with preset fractures under chemical solutions of different pH values (1, 3, 7, 12) and soaking days ($t = 5, 100$ d) were carried out. The influences of t , pH , and σ on the hydraulic properties of fractured rock masses were analyzed.

The fluid flow test results under different σ are consistent with the Forchheimer theoretical equation, and the fitting coefficients are all larger than 0.99. The difference between inlet and outlet pressure $-\Delta P$ decreases with an increase in σ . When σ increases from 0.5 MPa to 20 MPa, both the linear coefficient a and the nonlinear coefficient b in the Forchheimer equation show logarithmic increases, and b is 6 orders of magnitude larger than a . Under the same confining pressure conditions, the fluid flow characteristics of the granite fracture network in a neutral or acidic solution are most significantly affected by soaking time. When the solution is strongly acidic ($pH = 1$), the $-\Delta P$ at $t = 100$ d is 25% larger than that at $t = 5$ d. In a neutral solution ($pH = 7$), J_c remains relatively constant over time, showing little sensitivity to variations in t . In contrast, in both acidic and alkaline solutions ($pH = 1, 3$, and 12), J_c fluctuates significantly

with changes in both t and σ , indicating that the fluid flow behavior is highly influenced by the environment. The permeability coefficient K decreases with an increase in σ . When the solution is neutral, the influence of t on K is most obvious. Predictive equations for J_c and K of the fractured rock mass after chemical corrosion treatment was proposed, and the calculated values from these equations were compared with experimental results. The comparison results demonstrated a good fit between the two datasets. Therefore, the predictive equations for J_c and K , as proposed in this study, can provide theoretical guidance for the study of fluid flow through fractured rock masses subjected to chemical corrosion.

The proposed empirical equations for J_c and K can be applied to the fluid flow model of fractured rock masses under chemical corrosion, which is a crucial step in the calculation process. Many previous studies used the cubic law as the governing equation to solve fluid flow through a fractured network but applied a larger J than J_c calculated by Eqs. (14) or (16). The use of the N-S equations is appreciated for modeling fluid flow in each single fracture when J is larger than J_c , which, however, is not always applicable due to the limitation of computational capacities when a large number of fractures are involved in a model. To have confidence in using the cubic law in a fractured network, the assigned J needs to be first checked by comparing it to the predictions of Eqs. (14) and (16) before conducting further flow and mass transport simulations. If J is larger than J_c , the relationship between Q and J needs to be assessed by employing Forchheimer's law, which can significantly reduce the calculation time.

The present work uses fractures that are saw-cut with smooth surfaces, which is not the natural case, where the fracture surface is always rough. Therefore, in future works, we will focus on the nonlinear fluid flow properties of fractured rock masses containing rough fractures treated after chemical corrosion.

Acknowledgements

This study has been partially funded by Natural Science Foundation of China, China (Grant No. 52379113), and Natural Science Foundation of Jiangsu Province, China (Grant No. BK20211584).

Conflict of Interest

The authors declare that they have no conflict of interest.

References

1. WANG Z., LI W., QIAO L., LIU J., YANG J. Hydraulic properties of fractured rock mass with correlated fracture length and aperture in both radial and unidirectional flow configurations, *Computers and Geotechnics*, **104**, 167, **2018**.
2. AMINJAN K.K., ESCOBEDO-DIAZ J.P., HEIDARI M., RAHMANIVAHID P., KHASHEHCHI M., MILANI S.M., SALAHINEZHAD M. Comment on “DPMLES investigation on flow field dynamic and acoustic characteristics of a twin-fluid nozzle by multi-field coupling method”, *International Journal of Heat and Mass Transfer*, **217**, 124678, **2023**.
3. WANG F., ZHOU M., SHEN W., HUANG H., HE J. Fluid-solid-phase multi-field coupling modeling method for hydraulic fracture of saturated brittle porous materials, *Engineering Fracture Mechanics*, **286**, 109231, **2023**.
4. ASMOAY A.A., MABROUK W.A. Appraisal of rock-water interaction and frailty of groundwater to corrosion and salinization, northwestern Gulf of Suez, Egypt, *Journal of Umm Al-Qura University for Applied Sciences*, **1**, 1, **2023**.
5. AGUNG P., HASAN M., SUSILO A., AHMAD M., AHMAD M., ABDURRAHMAN U., SUDJIANTO A., SURYO E. Compilation of parameter control for mapping the potential landslide areas, *Civil Engineering Journal*, **9** (4), 2676, **2023**.
6. TAHIR Y., KADIRI I., FERTAHI S., YOUBI M., BOUFERRA R., AGOUNOUN R., DLIMI M. Design of controlled pre-split blasting in a hydroelectric construction project, *Civil Engineering Journal*, **9** (3), 2476, **2023**.
7. AMALUDIN A., ASRAH H., MOHAMAD H., AMALUDIN H., AMALUDIN N. Physicochemical and microstructural characterization of Klias Peat, Lumadan POFA, and GGBFS for geopolymer based soil Stabilization, *HighTech and Innovation Journal*, **4** (2), 2723, **2023**.
8. GAO G., CHEN J., HUO J. Effect of Different Corrosion Rates on the Seepage Dissolution Model of Single Fractures in Limestone, Yangtze River, **50** (10), 1, **2019**.
9. LAWRINENKO M., KURWADKAR S., WILKIN R.T. Long-term performance evaluation of zero-valent iron amended permeable reactive barriers for groundwater remediation—A mechanistic approach, *Geoscience frontiers*, **14** (2), 101494, **2023**.
10. LI B., YE X., DOU Z., ZHAO Z., LI Y., YANG Q. Shear Strength of Rock Fractures Under Dry, Surface Wet and Saturated Conditions, *Rock Mechanics and Rock Engineering*, **53**, 1, **2020**.
11. KESSLER D.W., INSLEY H., SLIGH W.H. Physical, mineralogical and durability studies on the building and monumental granites of the United States, *Journal of Research of the National Bureau of Standards*, **24**, 161, **1940**.
12. LUO J., ZHU Y., GUO Q., TAN L., ZHUANG Y., LIU M., ZHANG C., ZHU M., XIANG W. Chemical stimulation on the hydraulic properties of artificially fractured granite for enhanced geothermal system, *Energy*, **142** (1), 754, **2018**.
13. KAMALI-ASL A., GHAZANFARI E., PERDRIAL N. Effects of injection fluid type on pressure-dependent permeability evolution of fractured rocks in geothermal reservoirs: An experimental chemo-mechanical study[J]. *Geothermics*, **87**, 101832, **2020**.
14. FARQUHARSON J.I., KUSHNIR A.R.L., WILD B., BAUD P. Physical property evolution of granite during experimental chemical stimulation, *Geothermal Energy*, **8** (1), 1, **2020**.
15. DING W.X. and FENG X.T. Damage effect and fracture criterion of rock with multi-preexisting cracks under chemical erosion, *Chinese Journal of Geotechnical Engineering*, **31** (6), 899, **2009**.
16. LI H., ZHONG Z., ESHIET K.I., SHENG Y., LIU X., YANG D. Experimental investigation of the permeability and mechanical behaviours of chemically corroded limestone under different unloading conditions, *Rock Mechanics and Rock Engineering*, **53**, 1587, **2020**.
17. ZHOU X.-P., YU T.-Y. Experimental Study on the Dynamic Failure Behaviors of Granite After Chemical Corrosion, *Rock Mechanics and Rock Engineering*, **56** (11), 7923, **2023**.
18. SHANG D., ZHAO Z., DOU Z., YANG Q. Shear behaviors of granite fractures immersed in chemical solutions, *Engineering Geology*, **279**, 105869, **2020**.
19. SHENG J., GAO P., WANG K., GAO H., TIAN X. Experiments of seepage erosion influence on shear characteristics of rock fracture, *Advances in Science and Technology of Water Resources*, **41** (2), 42, **2021**.
20. HUANG Z., ZENG W., GU Q., WU Y., ZHONG W., ZHAO K. Investigations of variations in physical and mechanical properties of granite, sandstone, and marble after temperature and acid solution treatments, *Construction and Building Materials*, **307**, 124943, **2021**.
21. MENG X., MENG F., LI H., LI Z., PENG P. Analysis on non-Darcy flow characteristic for fractured rock, *The Chinese Journal of Geological Hazard and Control*, **21** (4), 1003, **2020**.
22. FU H., JIANG H., QIU X., JI Y. Seepage characteristics of single-fracture silty mudstone under low stress and overlying water environment, *Rock and Soil Mechanics*, **41** (12), 3840, **2020**.
23. BORDIER C., ZIMMER D. Drainage equations and non-Darcian modelling in coarse porous media or geosynthetic materials, *Journal of Hydrology*, **228** (3), 174-187, **2000**.
24. ZENG Z., GRIGG R. A criterion for non-Darcy flow in porous media, *Transport in porous media*, **63**, 57, **2006**.
25. ZIMMERMAN R.W., AL-YAARUBI A., PAIN C.C., GRATTONI C.A. Non-linear regimes of fluid flow in rock fractures, *International Journal of Rock Mechanics and Mining Sciences*, **41**, 163, **2004**.
26. WANG S., CHEN Y., ZHOU Q. Mechanical properties of granite under uniaxial compression induced by acid solution. *Chinese Journal of Geology*, **42** (04), 686, **2018**.
27. PAN J., CAI M., LI P. Uniaxial compressive damage constitutive model of rock-like materials with single fissure after chemical corrosion. *Journal of Central South University*, **29** (02), 486, **2022**.
28. MO Y., LIU J., LIU L. Corrosion behavior of rebar in cement-bagasse ash-mineral powder sea sand mortar. *Journal of silicate*, **51** (11), 2792, **2023**.

29. CUI X., ZHENG Z., ZHANG H., ZHANG C., LI X., ZHU P., CHEN Z. Impact of water-rock interactions on indicators of hydraulic fracturing flowback fluids produced from the Jurassic shale of Qaidam Basin, NW China. *Journal of Hydrology*, **590**, 125541, **2020**.
30. ZHANG L., HASCAKIR B. A review of issues, characteristics, and management for wastewater due to hydraulic fracturing in the US. *Journal of Petroleum Science and Engineering*, **202**, 108536, **2021**.
31. MOBASHER M.E., WAISMAN H. Energy dissipation mechanisms in fluid driven fracturing of porous media. *Geomechanics and Geophysics for Geo-Energy and Geo-Resources*, **8** (5), 157, **2022**.
32. WANG C., LU Y., HAO G., CUI B., ZHAO Z. Experimental study on deformation characteristics of fractured rock mass under water-rock action. *Water conservancy and hydropower technology*, **49** (05), 136, **2018**.
33. KUBRAKOVA I.V., TYUTYUNNIK O.A., SILANTYEV S. Mobility of Dissolved Palladium and Platinum Species during the Water–Rock Interaction in a Chloride Environment: Modeling of PGE Behavior during Interaction between Oceanic Serpentinites and Seawater Derivatives. *Geochemistry International*, **57**, 282, **2019**.
34. HU R., ZHOU C., WU D., YANG Z., CHEN Y. Roughness Control on Multiphase Flow in Rock Fractures. *Geophysical Research Letters*, **46**, 12002, **2019**.
35. SUN H., LIU X., YE Z., WANG E. A new proposed method for observing fluid in rock fractures using enhanced x-ray images from digital radiography. *Geomechanics and Geophysics for Geo-Energy and Geo-Resources*, **8** (1), 10, **2021**.
36. JIANG Z., JIANG A., LI H. Change law study on cut-through fracture seepage properties of slate in corrosion environment, *Journal of China Coal Society*, **41** (8), 1954, **2016**.